All-Electric X-Plane, X-57 Mod II Ground Vibration Test

Natalie Spivey[1], Samson Truong[1], and Roger Truax[1]

[1]Armstrong Flight Research Center
National Aeronautics and Space Administration
4800 Lilly Ave Edwards, CA 93523 USA

ABSTRACT
As part of the National Aeronautics and Space Administration New Aviation Horizons initiative to demonstrate and validate future high-impact concepts and technologies, the X-57 Maxwell airplane -- the first all-electric X-plane -- was conceived to advance research in the area of electric propulsion to show the feasibility of minimizing fuel use, reducing emissions, and lowering noise during flight. Through several configuration modifications to the X-57 airplane, validation of electrical-powered flight with increasing efficiency between each modification when compared to the baseline original airplane is anticipated. In the case of the X-57 Modification II airplane, a ground vibration test was needed to identify the airplane structural modes and use them to update and validate the finite element model. To determine the airworthiness of the airplane the updated finite element model will be utilized to investigate both classical and whirl flutter. The X-57 Modification II ground vibration test was performed by the National Aeronautics and Space Administration Armstrong Flight Research Center Flight Loads Laboratory. This paper will highlight the testing performed to acquire the modal data as well as the results.

Keywords: Electric, Ground Vibration Test, Modal, X-57 Airplane

NOMENCLATURE

A/C	=	aircraft
accel	=	accelerometer
AFRC	=	Armstrong Flight Research Center
ail	=	aileron
anti-sym	=	anti-symmetric
AW1T	=	anti-symmetric wing 1st torsion
AW1B	=	anti-symmetric wing 1st bending
AW2B	=	anti-symmetric wing 2nd bending
BCM	=	battery control module
CAD	=	computer-aided design
DOF	=	degrees of freedom
F1LB	=	fuselage 1st lateral bending
F1VB	=	fuselage 1st vertical bending
F/A	=	fore/aft
FEM	=	finite element model
FLL	=	Flight Loads Laboratory
GVT	=	ground vibration test
HL	=	high-lift
lat	=	lateral
long	=	longitudinal
MLG	=	main landing gear
Mod	=	modification
NASA	=	National Aeronautics and Space Administration
OOP	=	out of phase
rotn	=	rotation
SW1B	=	symmetric wing 1st bending

SW1T = symmetric wing 1st torsion
SW2B = symmetric wing 2nd bending
SWFA = symmetric wing fore/aft
sym = symmetric
TE = trailing edge
vert = vertical

1 INTRODUCTION

The X-57 Maxwell will incorporate a distributed electrical propulsion system and is derived from a modified baseline Italian general aviation fleet airplane called the Tecnam P2006T (Costruzioni Aeronautiche Tecnam, Capua, Italy).[1-2] The X-57 airplane is being redesigned over several configuration modifications in order to evaluate the performance to the original baseline airplane, as shown in figure 1. Modification (Mod) I is the baseline Tecnam P2006T airplane with two mid-wing gas powered engines; Mod II is Mod I redesigned with two electric motors powered by traction batteries, see figure 2. Mod IV will incorporate a new wing design with the two electric cruise motors moved to the wingtips and 12 high-lift (HL) electric motors, mounted and distributed along the wing leading edge; the previous Mod III configuration and objectives have been merged with the Mod IV configuration. The goal of the X-57 airplane project is to demonstrate a 500-percent increase in high-speed cruise efficiency, zero in-flight carbon emissions, and a 15-dB reduction in noise levels.

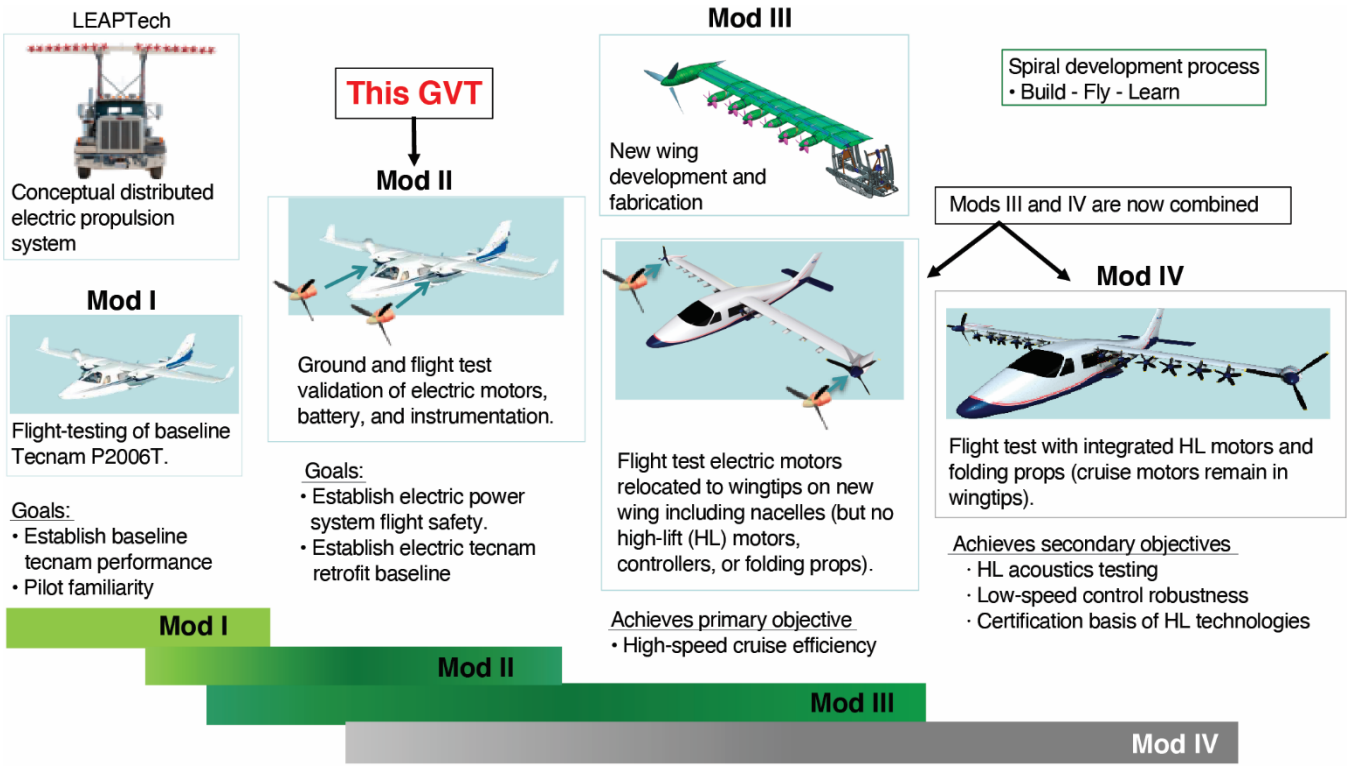

Figure 1: X-57 airplane project configuration modifications

Figure 2: X-57 Mod II airplane, artist illustration

The National Aeronautics and Space Administration (NASA) Armstrong Flight Research Center (AFRC) Flight Loads Laboratory (FLL) conducted a ground vibration test (GVT) on the X-57 Mod II airplane, as shown in figure 3, in order to gather modal data of a near flight-ready configuration to correlate and validate the Mod II airplane beam finite element model (FEM) to the airplane GVT modes.[3] After correlating the FEM to match the GVT data, the updated FEM will be used in both the final classical and whirl flutter analyses that will be used for evaluating aeroelastic airworthiness for the X-57 Mod II airplane flights. Two separate airplane boundary conditions were conducted. One setup was with the X-57 Mod II airplane on a soft-support system to simulate the free-flight boundary conditions. The second boundary condition tested was with the airplane on-tires to characterize the on-ground modes for future airplane ground motor testing safety clearance and potential follow-on of ground GVTs when the airplane will be taxiing on the runway. Multiple test configurations were conducted during the X-57 Mod II GVT, each configuration with a different target airplane structural mode of interest; these test configurations dictated which locking mechanisms were to be used in the cockpit and on the control surfaces. Locking devices are commonly used to constrain moving components during GVTs. A total of 191 test runs were performed for this Mod II GVT.

Figure 3: X-57 Mod II airplane ground vibration test setup on soft supports to simulate a free-free boundary condition

2 TEST OBJECTIVES

The purpose of the X-57 Mod II airplane GVT was to gather the modal frequencies and mode shapes of the airplane in a flight-ready configuration. The GVT will be used to correlate and validate the Mod II airplane FEM to that of the airplane GVT elastic modes. The resultant updated FEM will be utilized for flutter analysis predictions, which are critical for flight flutter envelope expansion.[4] The primary test objective and the main structural modes of interest during the GVT involved modes that are part of the predicted airplane flutter mechanism, see table 1. For classical flutter, the flutter mechanism was a concern because of the coupling of the horizontal stabilator rotation and the fuselage 1st vertical bending (F1VB) modes. For whirl flutter, the flutter mechanism and modes of concern were the motor assembly lateral bending and vertical bending.[5-6] In addition to the airplane elastic flutter mechanism modes, the airplane rigid-body modes were also part of the primary test objective, see table 1. The newly designed X-57 soft-support system needed to provide adequate frequency separation of the airplane elastic and rigid modes to avoid potential coupling. Frequency separation would characterize the effectiveness of the soft supports to simulate the airplane in a free-flight environment, which greatly simplifies the post-test FEM correlation to the GVT results. The remainder of the airplane elastic modes were either secondary or tertiary objectives and were not expected to contribute to the flutter mechanism. The secondary objective modes involved the fuselage lateral bending and torsion modes, wing modes, and landing gear modes. The tertiary modes were higher-order wing modes and control surface modes. Identification of the secondary and tertiary modal frequencies and mode shapes would help assess the response of the airplane compared to the FEM predictions.

Table 1: Primary objectives for the X-57 Mod II airplane ground vibration test

Primary Objectives

- Stabilator Rotation
- Fuselage 1st Vertical Bending

Modes in pre-test FEM predicted Classical Flutter Mechanism

- Motor Assembly Vertical Bending
- Motor Assembly Lateral Bending

Modes in pre-test FEM predicted Whirl Flutter Mechanism

- Aircraft Rigid Body Modes (Characterize Soft Support Effectiveness)

Two boundary conditions were evaluated to meet the objectives for the X-57 Mod II GVT. The first boundary condition setup had the airplane suspended on a soft-support system to simulate a free flight; the second boundary condition setup had the airplane on-tires resting on the hangar floor. The free-free setup utilized the newly designed X-57 soft-support system to simulate the airplane in free flight with essentially no boundary conditions interfacing or touching the airplane. This setup allowed an apples-to-apples comparison of the GVT data to the FEM free-free modal analysis, making the FEM updating and correlation process easier post-test. The updated FEM will be utilized in the flutter analysis to clear the Mod II airplane for flight. The flutter flight-testing team will also use the GVT results in the control room to assist in assessing the airplane modes during flight flutter envelope expansion clearance. The on-tires GVT configuration was intended to gather airplane modal data that would be utilized for several different reasons. The first reason was to obtain the baseline characterization of the motor assembly modes for safety clearance of near-term ground motor testing before flight. The second reason was to baseline the airplane on-tires modes in order to avoid the need to repeat a more complicated airplane GVT on soft supports (if needed) -- in case potential hardware changes before flight-testing raised flutter concerns that might not be alleviated or well predicted by FEM adjustments alone. The third reason was to gather modal data that would be comparable to low-speed airplane taxi testing as a buildup to higher-speed taxi testing and flight-testing.

3 TEST DESCRIPTION

The following sections describe the X-57 Mod II test article, the finite element model, and the details of the GVT. The X-57 Mod II airplane GVT was conducted from November to December 2019 at NASA AFRC.

3.1 Test Article

The X-57 Mod II airplane is a modified version of the Tecnam P2006T, an Italian general-purpose airplane with two all-electric motors and traction batteries in place of the factory gas motors. The electric motors were mounted onto motor adapters and the associated structural truss, which also houses the new cruise motor controllers. The motor truss assembly was attached to the existing firewall structure next to the wing leading-edge spar. Sixteen traction battery modules were used to power the twin electric motors and amount to nearly a third of the airplane total weight. The airplane configuration for the GVT contained power cables in the wing in addition to other flight instrumentation cables and sensors (flight accelerometers and strain gauges); all the components were installed before the airplane arrived at AFRC. The airplane weight (including all of the GVT locking devices, hardware, and ballast), was measured at 2,782 pounds prior to installing the GVT external accelerometers.

Because of safety concerns for the GVT, traction battery mass simulators were used in place of the energized batteries and were fabricated to be close in weight and center of gravity to the actual hardware. These traction battery mass simulators were mounted to the fuselage in the same fashion as their flight counterparts. The forward set of eight traction batteries was behind the pilot seat (previously the second row of seats in Mod I); the aft set of eight traction batteries was previously the cargo hold. Battery support equipment such as vent covers and hoses were also installed onto the mass simulators. Because two flight battery control modules (BCMs) were not ready in time for the GVT, two BCM mockup units (fabricated and mounted on the fuselage side wall behind the pilot seat) were used as alternates. The BCM mockup units were lighter than the actual units, so they were ballasted internally with shot bags to bring the weight to the expected BCM flight weights. The forward and aft traction battery setup inside the airplane is shown in figure 4.

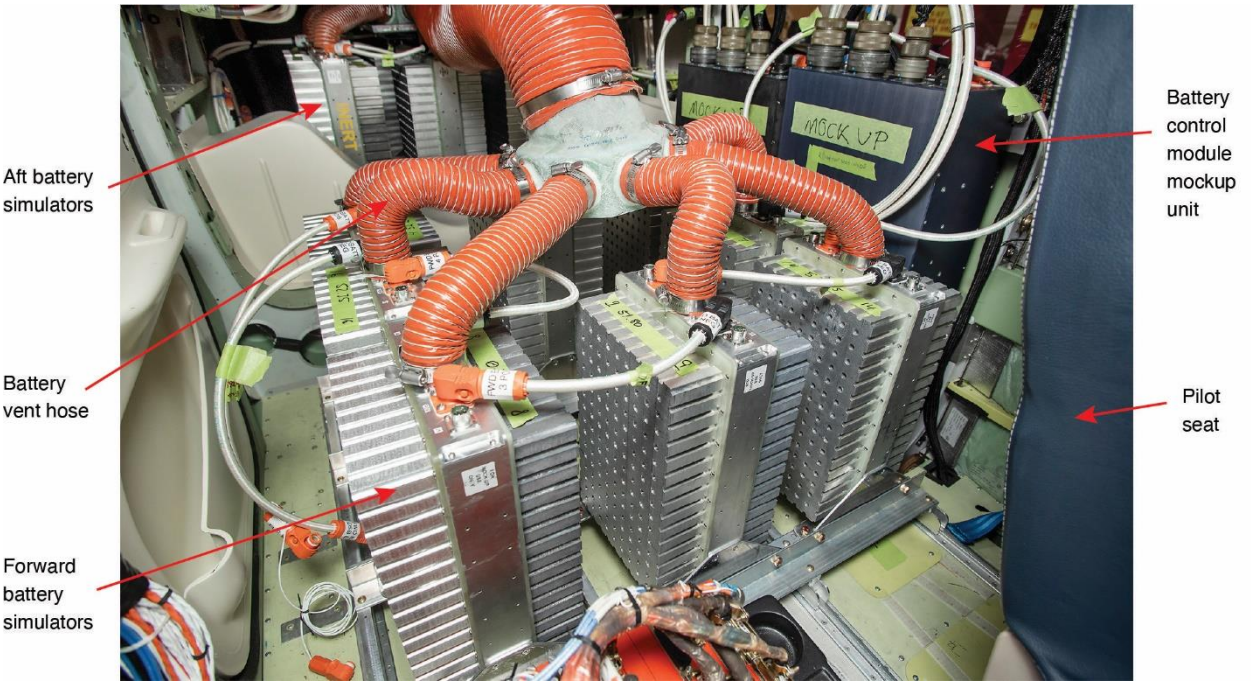

Figure 4: Battery simulator setup inside the cockpit for the X-57 Mod II airplane ground vibration test

Locking devices are commonly used to constrain moving components during GVTs which can dominate the desired structural modes. Locking devices used in this GVT were rudder and aileron gust locks, stabilator (stab) counterweight blocks, and yoke/pedal locks. The locking devices were used to constrain motion on the control surfaces and stabilator, depending on the particular tests that were run, in order to isolate a specific mode. For example, rudder and aileron gust locks, as shown in figure 5, were used to constrain motion of these surfaces to clearly identify primary airplane structural elastic modes. The control surface locks were standard airplane issued 4-in diameter outer (stiff plastic) and inner (foam) gust locks. The control surfaces were unlocked when the target mode of interest involved any control surface rotation. Table 2 (shown in section 3.6 Test Configurations) will show the details of the locking devices used per test configuration.

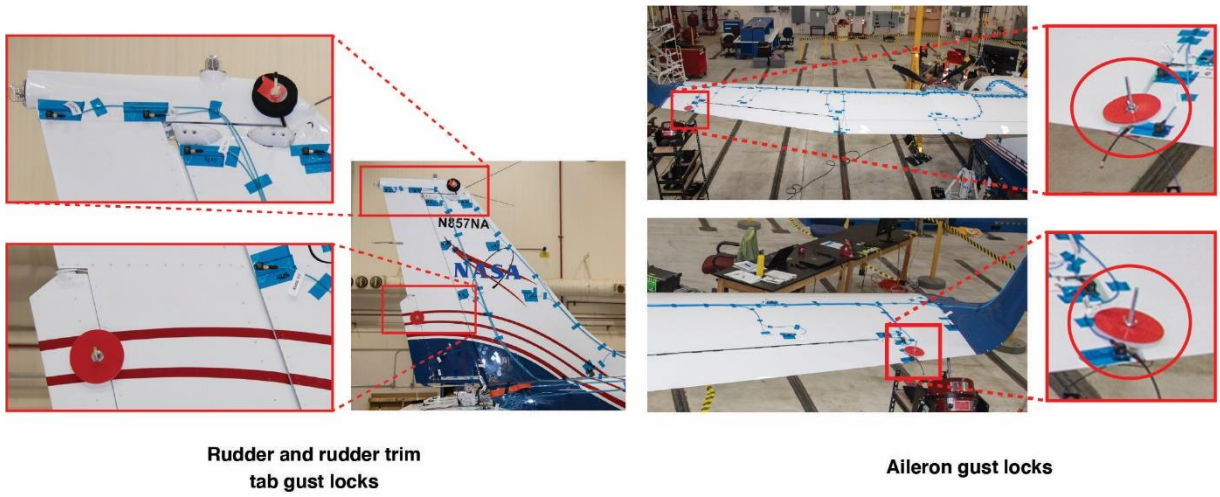

Figure 5: Rudder and aileron gust locks used for constraining these control surfaces

Several test configurations used a wooden stab counterweight block to simulate the stabilator as it would be positioned for steady-level flight when counteracting the aerodynamic forces. The majority of the test configurations had the stab

counterweight removed which caused the stabilator trailing edge to rotate down slightly. Gust locks were also used to constrain the stabilator trim tab in place, unless the stabilator was the mode of interest. The stab counterweight block and the stabilator trim tab gust lock locations are shown in figure 6. Because of the small size of the stab counterweight block and the installed location, where view was obstructed, a red “Remove Before Flight” tag was attached to the counterweight block for easy identification.

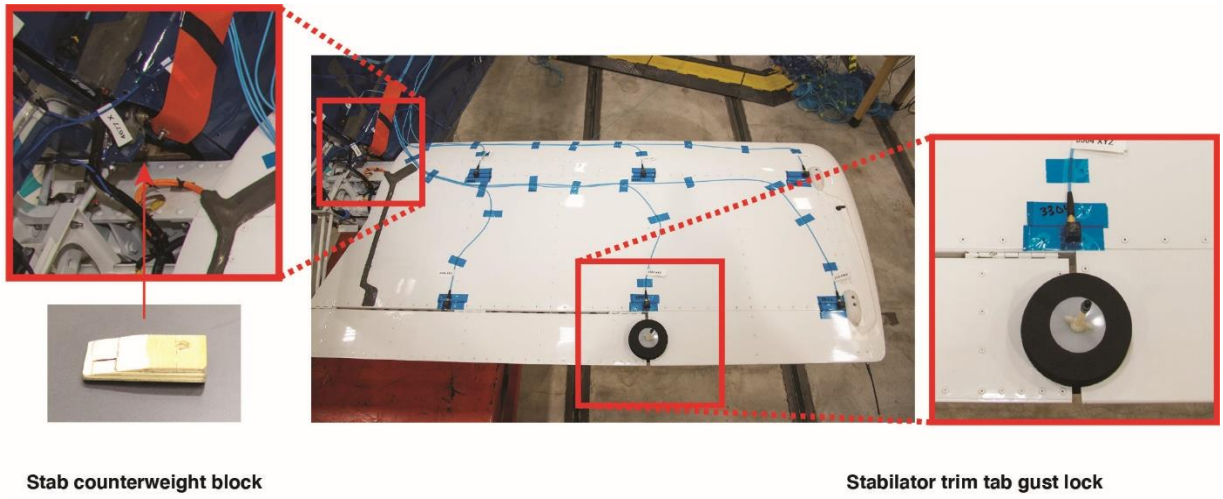

Figure 6: Location of stab counterweight block and stabilator trim tab gust lock

For this GVT, yoke and pedal locks were installed in the cockpit to simulate pilot contact with these components for steady-level flight and to prevent motion in the control surfaces. Figure 7 shows the yoke lock secured with two wooden boards installed in the cockpit and the 185-lb shot bag ballast on the pilot seat -- used to simulate the weight of the pilot. The pedal locks are hidden from view in the figure 7.

Figure 7: Yoke locks and pilot ballast setup inside the cockpit for the X-57 Mod II ground vibration test

3.2 Finite Element Model

The X-57 Mod II FEM was used for modal and flutter analysis predictions (pre-GVT planning), will be correlated to post-GVT results and can be used in both the classical and whirl flutter analyses. The airplane primary structure, control surfaces, and electric motors are modeled by elastically equivalent beams (blue lines) while retaining the same mode shapes and frequencies, as shown in figure 8. The motor adapter is represented by elastic solid elements (pink lines). The motor mount truss is modeled by elastic beams (green lines) that are attached with rigid beams (orange lines) to the wing equivalent beam, shown on each side of the wing. The wing and fuselage are connected with a rigid beam (orange line). The X-57 Mod II FEM is a highly-modified version of the original Tecnam P2006T flight test prototype airplane that was provided by the manufacturer. The airplane geometry was altered to represent the longer wingspan and increased vertical tail sweep of the fleet airplane that NASA is using for the X-57 airplane. Massless stiff elements (black lines) have been added to the equivalent elastic beams, leaving the airplane dynamically unchanged; these elements extend at near right angles from the elastic equivalent beams out to the planform edges for mode shape visualization and flutter analysis splining. Component structural and non-structural masses were extensively revised to reflect the distribution and center of gravity of the X-57 Mod II project computer-aided design (CAD) model. These revisions included the removal of the fleet airplane gas motors, fuel tanks, fuselage interior furnishings, and the addition of the electric motors, traction batteries, electric power controllers, wiring, and flight test equipment. The numerous point masses with their associated mass moment of inertias are not shown in figure 8. After the GVT, the X-57 Mod II FEM will be further updated to correlate and match the GVT results. This paper does not compare GVT results to the pre-test FEM.

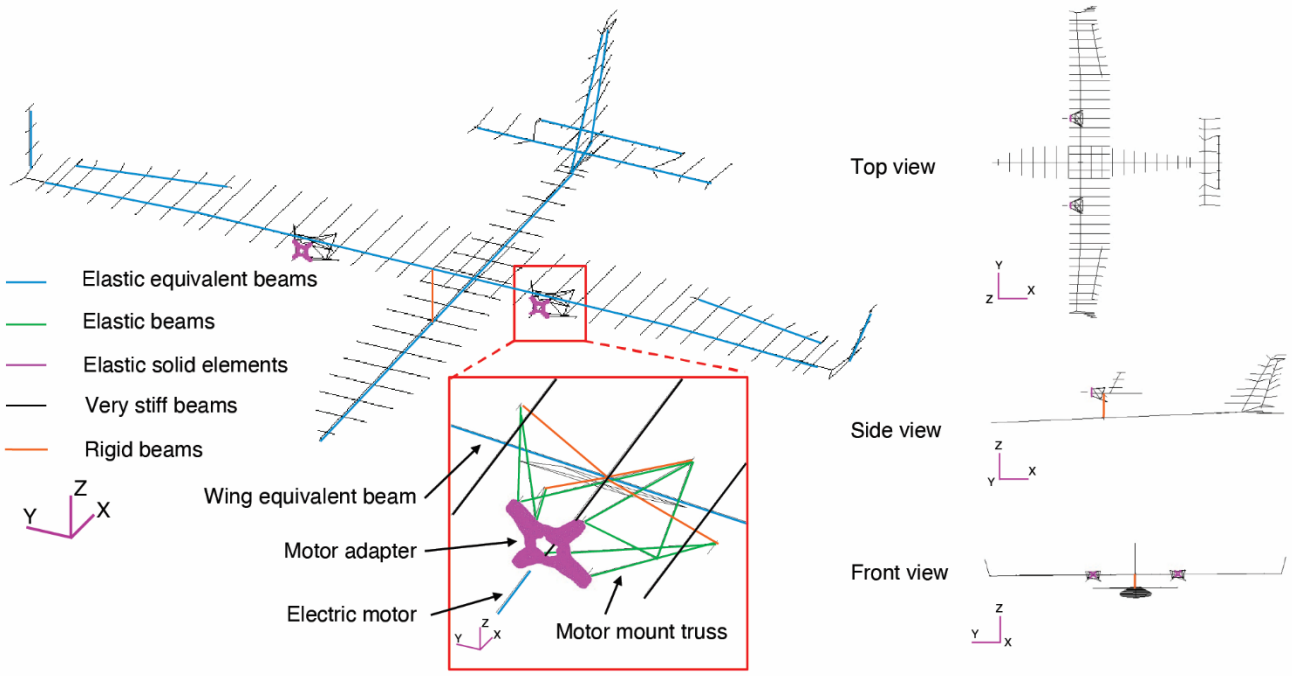

Figure 8: Finite element model of the X-57 Mod II airplane

3.3 Ground Vibration Test Setup

Two main boundary conditions were tested for the X-57 Mod II GVT. The first boundary condition setup had the airplane suspended on a soft-support system to simulate a free-flight environment; the second setup had the airplane on-tires resting on the hangar floor. These two different boundary conditions were used to obtain modal information in preparation for upcoming ground motor testing before flight, taxi tests, and Mod II flights. For ease of access for GVT accelerometer installation and removal of local modes, several additional items were removed from the airplane for the entire test: the nose panel, the stabilator tail cone, and an equipment pallet cover. In addition, characterization of the electric motors was essential

for this GVT and needed to be instrumented with accelerometers, so the motor fairings were removed as well. All of the items removed were weighed, and any missing weight will be accounted for in the post-test FEM updates.

3.3.1 Airplane on Soft Supports

For the free-free setup, a bungee-based soft-support system was designed by NASA AFRC utilizing standard airplane ground support equipment to suspend the airplane at underside airplane hard points.[7] Figure 9 shows the X-57 soft-support CAD design. The airplane landing gear was extended during testing to interface the main landing gear (MLG) with the soft-support system. The airplane was suspended at three points: two primary bungee lifting points (supporting the MLG axles), and a forward bungee lifting point (placed around the nose gear bulkhead by a lifting strap), supported by a 2-ton A-frame. To interface the bungees with the MLG axles, the following components were removed from the airplane for the test: the wheels, landing gear doors and associated pushrods and links. Two 5-ton tripod jacks Regent Model 985S (ColumbusJACK/Regent, Columbus, Ohio) were positioned on each side of the airplane around the axle and interfaced to the MLG soft-support beam. Three bungee loops were then linked between the jack soft-support beam to the axle on the MLG. This MLG soft-support setup was duplicated on both axles. The airplane was elevated each morning for testing through a coordinated series of jacking operations at the MLG soft-support jacks.

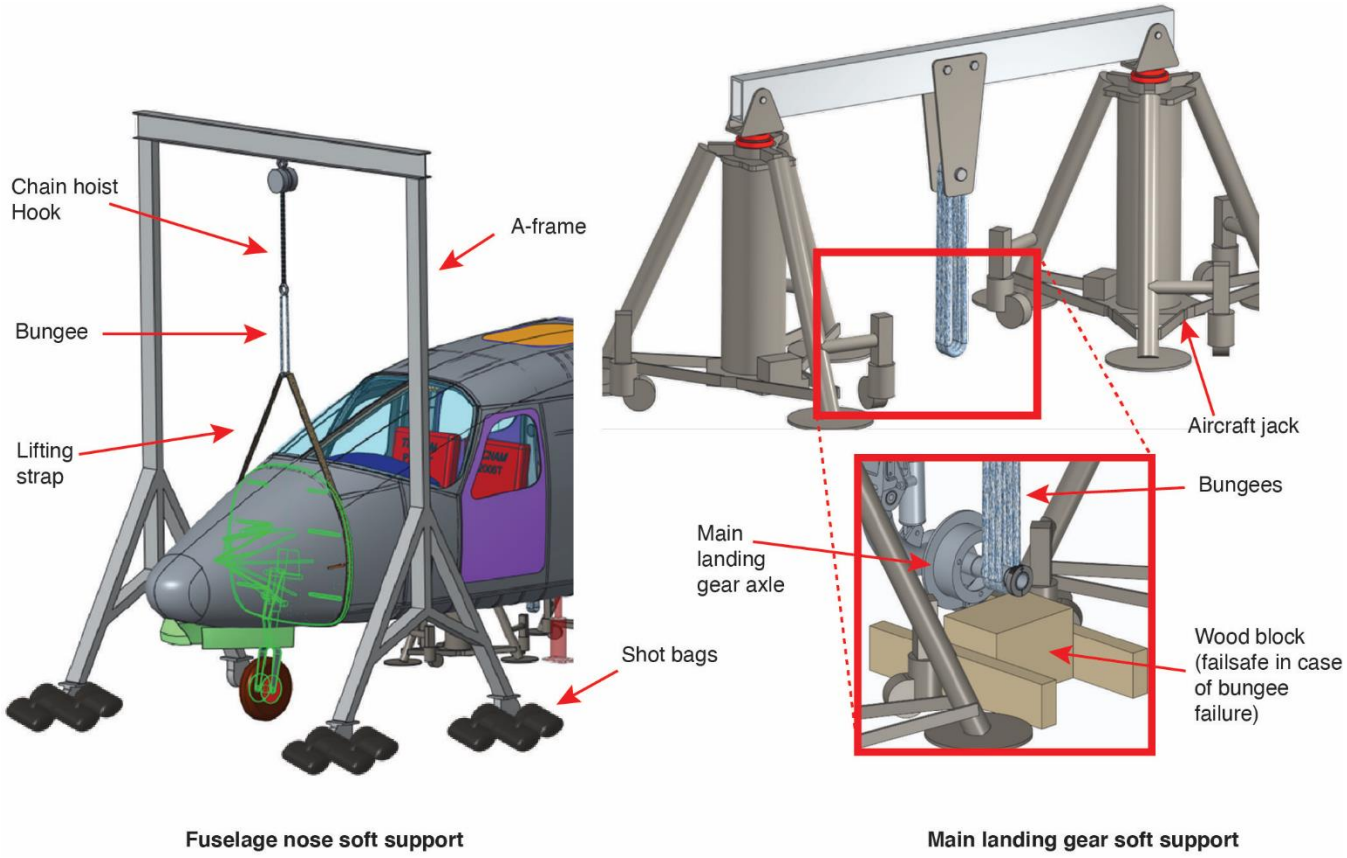

Figure 9: Computer-aided design of the newly designed X-57 soft-support system

The bungees used were 1080HD manufactured as continuous rings or loops and conformed to MIL-C-5651B, Type II bungee specifications; the HD in the bungee part number means “heavy duty.” Most HD bungee rubber is manufactured using a cut-tape method, as opposed to an extruded method. Cut-tape rubber bungees have a better low-frequency range over a wider-applied load range and are well-suited for GVT applications. Prior to the GVT, numerous bungee loops were tested and characterized to ensure a proper bungee selection that could both handle the load and have a low enough frequency response to ensure separation from the first airplane modal frequency. To suspend the fuselage nose, a lifting strap was wrapped around the nose gear bulkhead that was linked by a single bungee loop to a chain hoist and then connected to the yellow A-

frame lifting device. A piece of soft high-friction material was placed in between the lifting strap and fuselage surface to guard against slippage onto the thin airplane skin. The A-frame wheels were locked, and shot bags were placed at the wheels to constrain the A-frame from moving. When the airplane was suspended on soft supports, the nose gear wheel was approximately 1-2 in off the ground for testing. Figure 10 shows a close-up view of the soft-support system designed for this airplane GVT. The bungees were sturdy and never replaced throughout the test. The bungee soft-support lifting operations were extremely efficient and only took around 10 minutes at the beginning and end of each test day. Because of the way the Mod II airplane was suspended, the newly designed soft-support system eliminated the need for an overhead crane system and a critical lift procedure -- both of which would have required extra personnel and additional pre-GVT testing.

Figure 10: The soft-support system used for the free-free boundary condition setup

3.3.2 Aircraft On-Tires

The on-tires setup was the other boundary condition for this GVT and was performed after the free-free portion of the test. The airplane had its MLG wheels reinstalled and was then lowered to rest on the ground. All soft-support equipment was then moved out of the way for the remaining duration of the test. The on-tires testing had both normal service pressures in the tires (42 psi) and struts (nose: 130 psi, MLG (left and right): 320 psi). The airplane crew performed a shakedown of the airplane nose, tail, and wingtips to allow the struts to settle at equilibrium prior to testing. Chock blocks were removed from the tires prior to testing on the airplane. The on-tires setup for this airplane is shown in figure 11.

Figure 11: On-tires boundary condition setup

3.4 Ground Vibration Test Instrumentation

Three different types of accelerometers were used for this GVT: PCB T356A16, PCB T333B32, and PCB T333B (PCB Piezoelectronics, Depew, New York). The PCB T356A16 was used for triaxial measurements, and the PCB T333B32 and the PCB T333B for uniaxial measurements. For locations requiring measurements on two axes, two uniaxial accelerometers were installed in the orientation of the axes that needed measurement. Electromagnetic Modal 110 shakers (MB Dynamics, Cleveland, Ohio) were used mainly for random excitation. Depending on the target mode of the test configuration, either one or two shakers were used for that particular run.

The data acquisition (DAQ) LAN-XI DAQ hardware system (Brüel & Kjær, Nærum, Denmark) was used for this test. Four mainframes were used, two of the LAN-XI 11-slot main frame near the nose of the airplane (where the main GVT control station was located) and two of the LAN-XI 5-slot main frame at the rear of the airplane. The mainframes were daisy-chained together via a network switch. The LAN-XI modules were contained within each mainframe where the force transducers for the shakers and all the accelerometers would be connected (one axis per channel).

3.5 Ground Vibration Test Accelerometer Layout

The X-57 Mod II GVT included external accelerometers distributed along both sides of the airplane fuselage, wing spars, control surfaces, motors, and soft-support frames (located at the MLG and the fuselage nose). A total of 127 accelerometer locations measuring 318 degrees of freedom (DOF) were configured for the free-free setup; all accelerometers where installed using the global coordinate system of the airplane. For the on-tires setup, all accelerometers associated with the soft-support system were removed and disconnected from the DAQ, leaving a total of 113 accelerometer locations measuring 276 DOF. For both setups, a combination of uniaxial and triaxial accelerometers were installed, but the majority of the accelerometer locations were dual DOFs; either two uniaxial accelerometers or two DOFs from the triaxial accelerometer were used. Figures 12, 13, and 14 detail the GVT accelerometer layout for this test from different vantage points. It should be noted that the suite of accelerometers installed around the motors were very difficult to install because of the limited access and real estate around the electric motors. In addition to the GVT external accelerometers, flight accelerometer data were acquired near the end of the test using the airplane instrumentation system. As an initial way to evaluate the flight accelerometers, post-test comparisons of the flight accelerometers time and frequency responses to the nearest co-located GVT accelerometers will be performed.

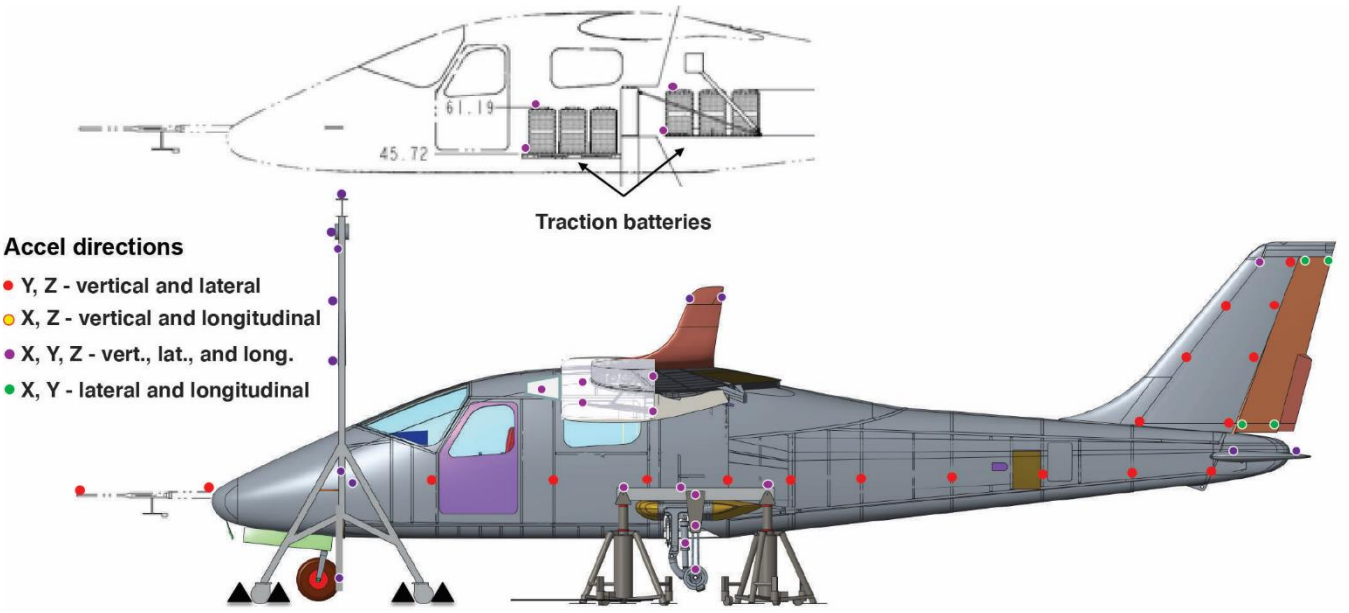

Figure 12: Ground vibration test accelerometer layout for X-57 Mod II airplane (side view)

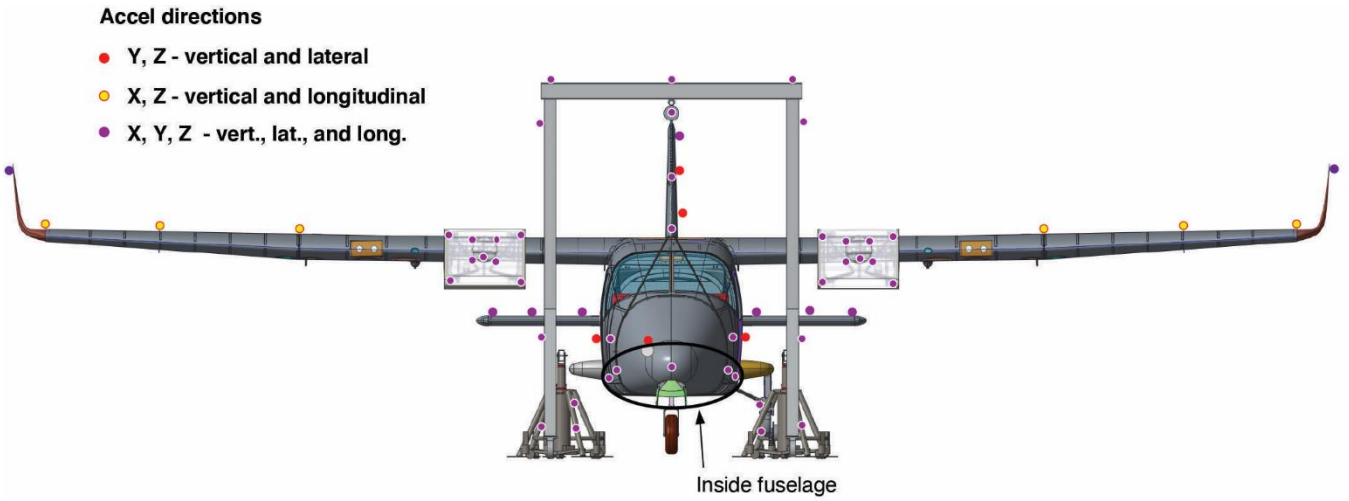

Figure 13: Ground vibration test accelerometer layout for X-57 Mod II airplane (front view)

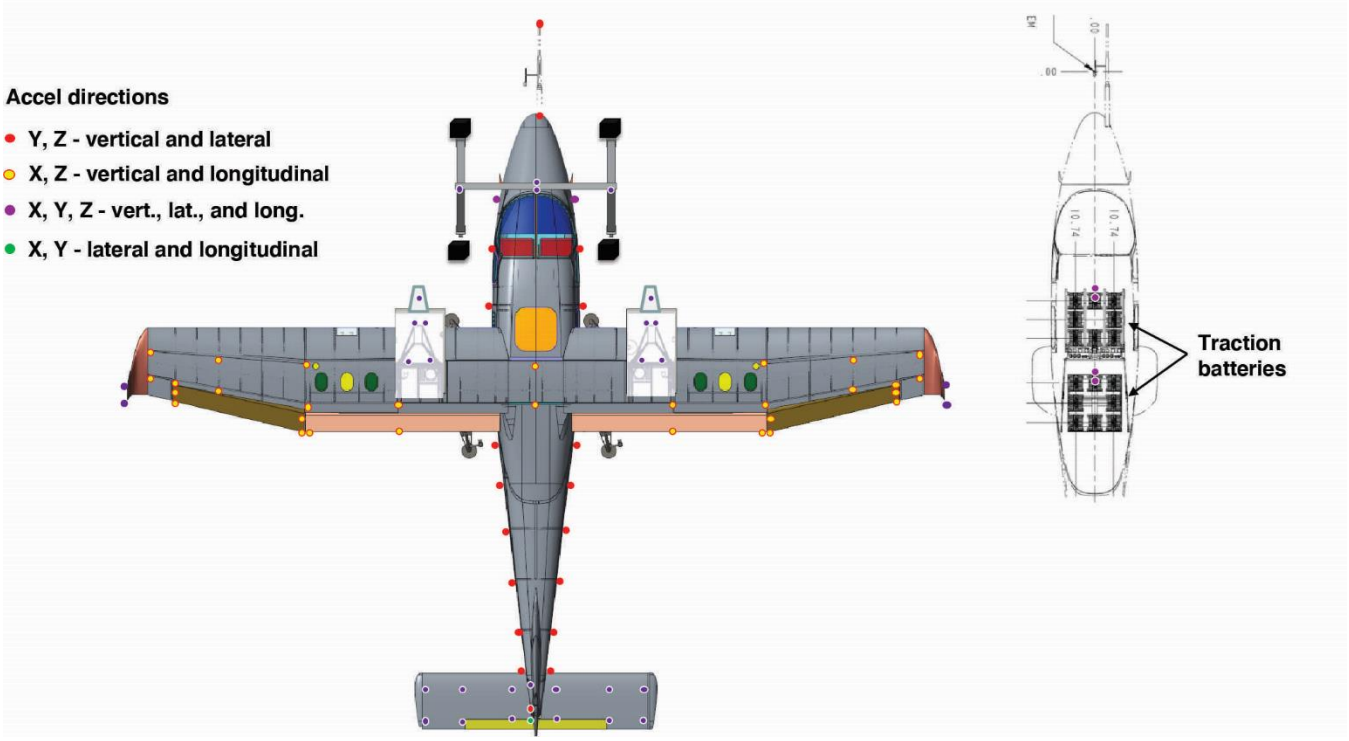

Figure 14: Ground vibration test accelerometer layout for X-57 Mod II airplane (top view)

3.6 Test Configurations

A total of 14 test configurations were performed for the X-57 Mod II GVT, 11 for the free-free soft-support setup and two for the on-tires setup. An additional last-minute test configuration was performed by exciting directly on the A-Frame lifting device interfacing to the nose soft support to characterize the A-Frame and ensure there was no coupling with the airplane modes of interest. The airplane remained suspended on soft supports for this A-Frame test. Table 2 details the test configuration matrix, including the target modes, excitation locations and directions, number of shakers, and which locking devices were used as constraints in either the cockpit or the control surfaces. The last column in the table shows the stab counterweight constraint either on or off. A few test configurations had both stab counterweight “on/off”, so those configurations had separate test runs depending on whether the stab counterweight was installed or not. Throughout the testing, the test engineers relied heavily on this configuration matrix to ensure both primary and secondary test objectives were achieved. Figure 15 shows some, but not all, of the various shaker locations that were positioned for the many test runs that were performed.

Table 2: Test configuration matrix for the X-57 Mod II airplane ground vibration test

Setup	Significance	Objective Mode(s)	Excitation Location(s) & Direction	Excitation Type	Cockpit Controls	Gust Locks	Stab Counterweight
Free-Free on Soft Supports	Primary	A/C Rigid Body	Fuselage/Wing	Manual Push	Yoke & Pedals Locked	Aileron & Rudder	On
	Primary	Stab Rotation	Aft Fuselage Vert	1 Shaker	Yoke & Pedals Locked	Aileron & Rudder	On/Off
	Primary	Stab Rotation	Aft Fuselage Lat, 30° Vert / 60° Lat	1 Shaker	Yoke Free, Pedals Locked	Aileron & Rudder	On/Off
	Primary	Fuselage Vert/Lat	Aft Fuselage Vert	1 Shaker	Yoke & Pedals Locked	Aileron & Rudder	On/Off
	Primary	Motor Vert/Lat	Prop Hub Vert, 45° Sym/Anti-Sym	2 Shakers	Yoke & Pedals Locked	Aileron & Rudder	On
	Secondary	Wing Bend, F/A, & Torsion	Wingtip TE Vert, 60° Vert / 30° F/A (Sym & Anti-Sym)	1 or 2 Shakers	Yoke & Pedals Locked	Aileron & Rudder	On
	Secondary	Fuselage Torsion & Vert Tail Bend	Vertical Tail Lateral	1 Shaker	Yoke & Pedals Locked	Aileron & Rudder	On/Off
	Secondary	Main Landing Gear	MLG Lat, 45° Lat	2 Shakers	Yoke & Pedals Locked	Aileron & Rudder	On
	Tertiary	Aileron Rotation	Wingtip TE 60° Vert / 30° F/A (Sym & Anti-Sym)	2 Shakers	Yoke & Pedals Locked	Rudder	On
	Tertiary	Rudder Rotation	Vertical Tail Lateral	1 Shaker	Yoke & Pedals Locked	Aileron	On
	Secondary	A/C Modes	Repeat ideal excitation locations	1 or 2 Shakers	Yoke & Pedals Locked	None	Off
On Tires	Secondary	A/C Taxi Modes & Flt Accels	Repeat ideal excitation locations	1 or 2 Shakers	Yoke & Pedals Locked	None	Off
	Primary	Motor Vert/Lat	Prop Hub Vert, 45° Sym/Anti-Sym	2 Shakers	Yoke & Pedals Locked	Aileron & Rudder	On
A-Frame Test	Tertiary	A-Frame	Vert Beam Lat, 30°Lat / 60° Long	2 Shakers	Yoke & Pedals Locked	Aileron & Rudder	On

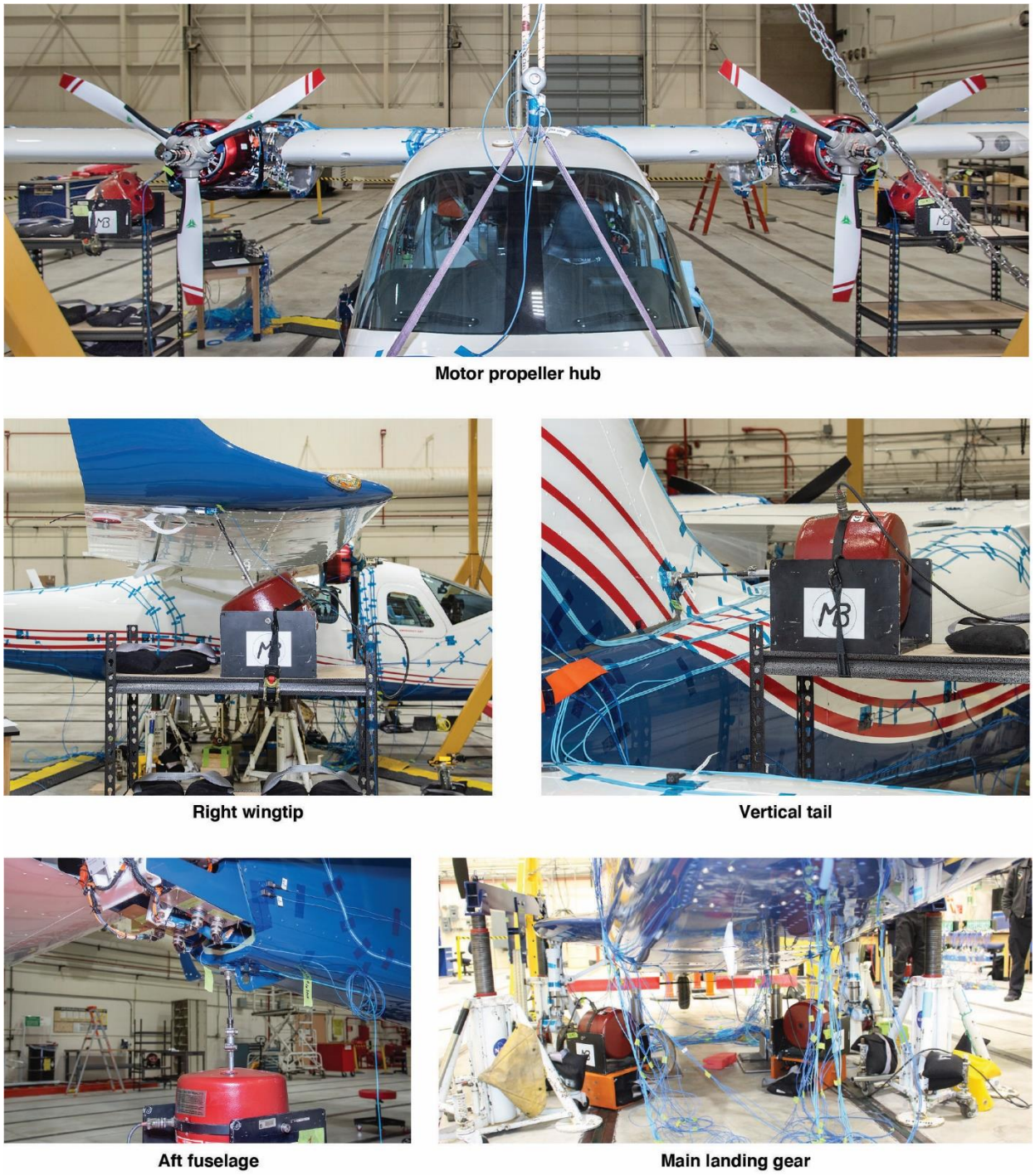

Figure 15: Various shaker locations for the X-57 Mod II airplane ground vibration

4 RESULTS

A total of 191 test runs were performed during the X-57 Mod II airplane GVT. Data were acquired using BK Connect® Version 19 software (Brüel & Kjær, Nærum, Denmark). The following sections show the modal test results for the airplane in both free-free and on-tires boundary conditions, as well as the results for the motors and the airplane rigid-body modes. It should be noted that because of the proprietary nature of the original Tecnam P2006T airplane FEM, pre-test analytical

predictions compared to the Mod II GVT results are limited. Once the X-57 Mod II FEM is correlated to the GVT results, post-test FEM versus GVT comparison will be made at a later date.

4.1 Test Display Model

The test display models or GVT models for visualizing the test mode shapes were created in BK Connect® software prior to testing using a combination of quadrilateral and triangular elements connecting the GVT external accelerometer locations on the airplane. The elements were grouped and color coded in the model to represent different parts of the airplane. An overall view of the test display model is shown in figure 16. Because only two accelerometers were connected, some airplane components and soft-support components are represented with trace lines instead of elements, as shown in figure 17. These airplane components included the nose boom, the main landing gear, and the forward and aft traction batteries in addition to the fuselage nose A-Frame soft support and the two MLG soft supports.

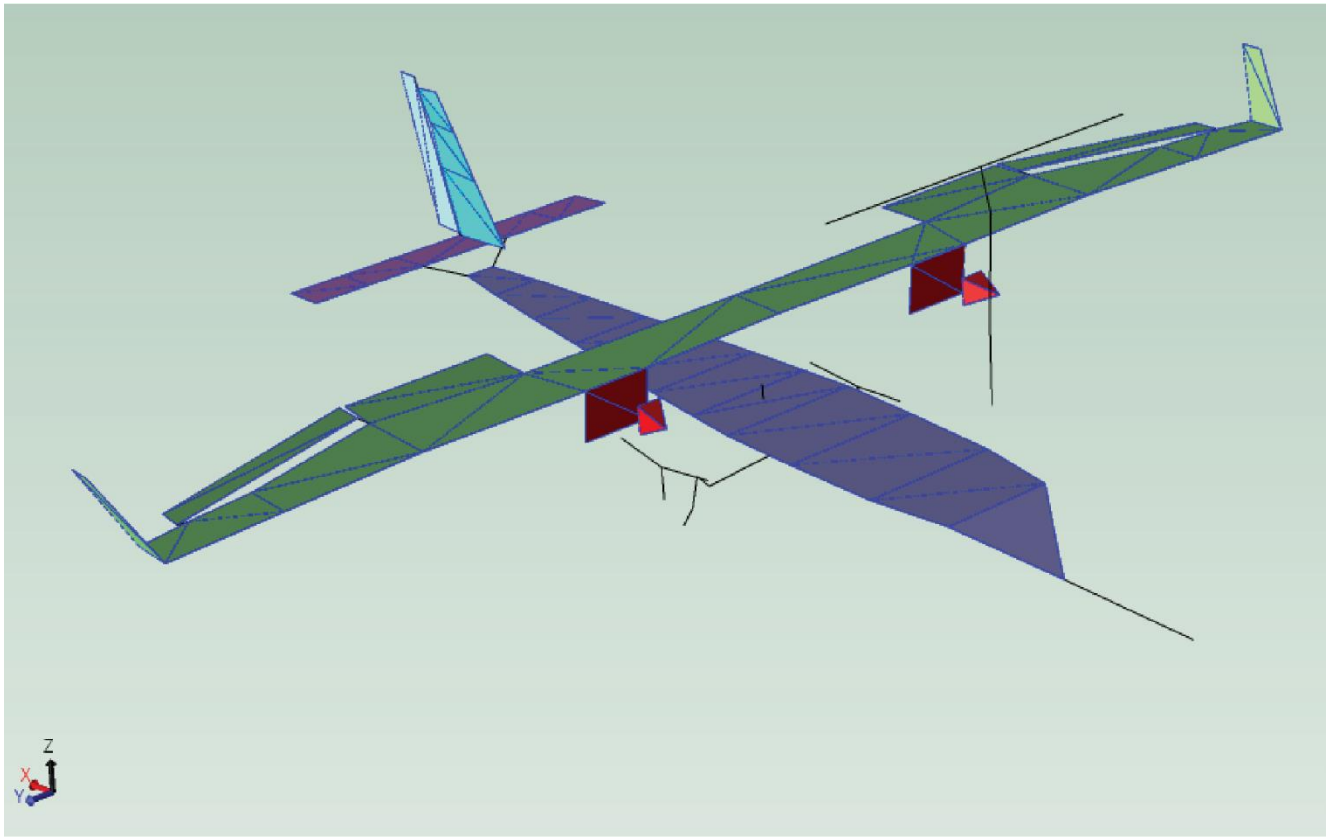

Figure 16: Test display model used for visualizing X-57 Mod II ground vibration test mode shapes

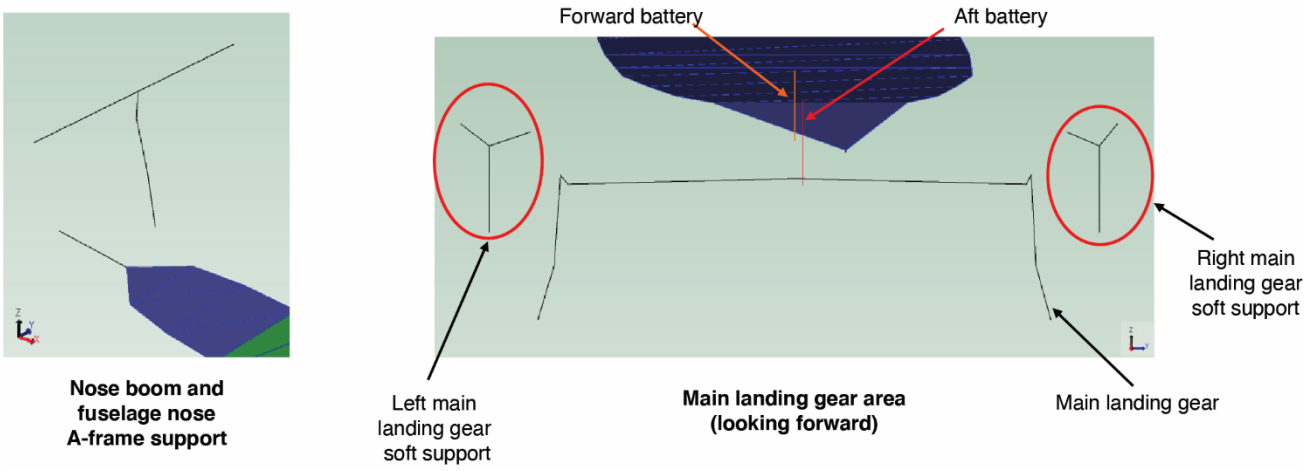

Figure 17: Close-up view of test display model components represented via trace lines

A second model was created post-test to better visualize and understand the behavior of the electric motor modes, particularly to see if there were any higher-order bending motor motions in either the lateral or vertical directions. Additional elements were added to connect the four accelerometers on the aft portion of the motor, known as the firewall, to the four accelerometers on the forward portion of the motor mount for both the left and right motors. This model is shown in figure 18.

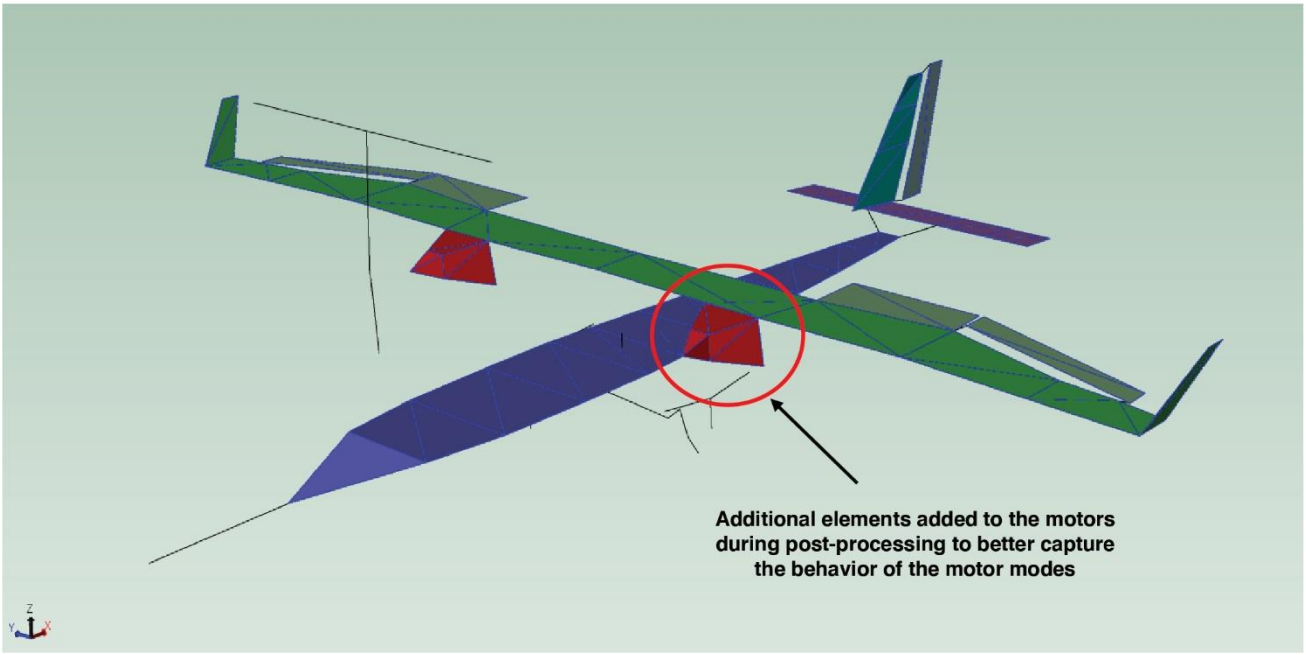

Figure 18: Test display model used for visualizing ground vibration test motor mode shapes

4.2 Airplane Results

The airplane results discussed in this section will focus on comparison of the two main setups, free-free and on-tires. For both setups, the airplane was configured with the stab counterweight block removed from the airplane; cockpit locks remained on the yoke and pedals. In addition, the gust locks were installed on the ailerons, rudder, and stabilator, exceptions for the removal of these components were only made during test runs when wanting to excite that particular control surface mode shape; for example, the rudder and rudder trim tab gust locks were removed for test runs targeting the rudder mode. Post-processing of the GVT results was performed in BK Connect® software with different parameter estimation techniques, but

predominantly using the polyreference time domain method.[8-9] The polyreference time domain method within the software application allows users to dictate how much time (decay time) after the peak response to include in the curve fit calculation.

The GVT results showed there were many airplane modes that appeared during the test but did not show up in the pre-test Mod II FEM modal results. Table 3 below shows the GVT elastic modal results for both the free-free and on-tires setups with the mode shapes listed in order of how they appeared in the free-free setup. Modes in blue text indicate that they were not seen in the pre-test FEM, most of which involved coupled airplane motion, wing torsion, and the control surfaces. In addition, the pre-test FEM did not model some components such as the nose boom; hence, these components were missing from the FEM. These missing FEM modes identified during the GVT will assist with the post-test model updating and correlation process. One should anticipate that the modal characteristics of the airplane with two different boundary conditions would be slightly different. Most modal frequencies between the free-free and on-tires setups were within ± 5 percent of one another. Note that some GVT modes for the on-tires setup are not in the order of the free-free setup; for example, the vertical tail bending mode is much higher for the on-tires setup at 17.41 Hz, whereas the free-free setup is at 15.98 Hz. Modes from the on-tires setup that exceeded a magnitude of 10-percent difference when compared to the free-free setup included the symmetric wing 2nd bending (SW2B) and the anti-symmetric aileron rotation modes. In addition, there were four modes that appeared in the free-free setup that were not present in the on-tires setup that included the two symmetric aileron rotation modes, rudder 2nd rotation, and symmetric flap rotation. Furthermore, there were a few modes in the free-free case that exhibited distinct or uncoupled shapes at certain frequencies but were coupled together for the on-tires case. For example, the anti-symmetric wing 2nd bending (AW2B) and the anti-symmetric aileron rotation modes at 20.69 Hz and 27.12 Hz, respectively, for the free-free results were rather coupled together for the on-tires results at 20.92 Hz. Similarities also occurred for the free-free case with the symmetric wing 2nd bending (SW2B) at 24.13 Hz and the stabilator bending/rotation mode at 28.47 Hz, but both of these modes coupled at 27.04 Hz in the on-tires case. For the on-tires case (in these instances) the modes were not seen as independent stand-alone modes as was seen in the free-free case.

Table 3: Frequency comparison table between free-free and on-tires ground vibration test setups. Mode names highlighted in blue were not predicted with pre-test finite element model and frequency differences of over five percent are highlighted in red

#	Free-Free Mode Name (in order of GVT)	GVT Free-Free Stab Off Frequency (Hz)	GVT On Tires Stab Off Frequency (Hz)	% Difference from GVT Free-Free Stab Off
1	Sym Wing 1st Bending (SW1B)	7.83	7.99	1.97%
2	Tail Roll with Anti-Sym Wing 1st Bending (AW1B)	9.06	9.56	5.56%
3	Stab Roll/Yaw with Fuselage 1st Lateral Bending (F1LB)	10.46	10.59	1.27%
4	Stab Roll/Yaw	11.51	11.71	1.73%
5	Rudder Rotation	12.67	12.70	0.25%
6	Stab Rotation	14.17	14.17	-0.02%
7	Anti-Sym Wing 1st Torsion (AW1T)	14.91	14.87	-0.27%
8	Vertical Tail Bending with Stab Roll	15.98	17.41	8.95%
9	Sym Wing 1st Torsion (SW1T)	16.79	16.96	1.00%
10	Sym Aileron Rotation with Rudder Rotation	16.95	17.21	1.54%
11	Sym Wing Fore/Aft (SWFA)	17.55	15.85	-9.72%
12	Fuselage 1st Vertical Bending (F1VB)	19.11	20.06	4.99%
13	Sym Aileron Rotation with Stab Bending	20.02	N/A	N/A
14	Anti-Sym Wing 2nd Bending (AW2B)	20.69	20.92	1.13%
15	Nose Boom Lateral	23.56	23.69	0.55%
16	Sym Wing 2nd Bending (SW2B)	24.13	27.04	12.07%
17	Nose Boom Vertical	26.49	26.44	-0.19%
18	Anti-Sym Aileron Rotation	27.12	20.92	-22.86%
19	Sym Aileron Rotation out-of-phase with Sym Flap/SW2B	27.64	N/A	N/A
20	Stab Bending/Rotation with winglet motion	28.47	27.04	-5.00%
21	Rudder Rotation/Torsion	29.37	N/A	N/A
22	Anti-Sym Winglet Bending (Rt Winglet Dominant)	30.36	30.14	-0.74%
23	Sym Winglet Bending (Rt Winglet Dominant)	31.68	31.61	-0.21%
24	Stab Rotation with Sym Stab Bending	34.15	34.18	0.07%
25	Sym Flap Rotation	34.40	N/A	N/A
26	Anti-Sym Flap Rotation	38.17	35.24	-7.68%

The resultant airplane mode shapes indicate there are some asymmetries between the left and right sides of the X-57 Mod II airplane; one side would likely be more dominant in response compared to its counterpart on the other side. This behavior is more pronounced on the control surfaces. Figure 19 and table 3 both show the GVT mode shapes and frequencies for the

free-free stab counterweight off setup; these modes will be used for the FEM updating process. Notice that for the last two modes, one flap is dominantly responding; the other flap is weak in response. The response is suspected from slight differences in the flap connections because of similarities in the right and left shaker forces. For the symmetric flap rotation mode, the right flap response is more evident; for the anti-symmetric flap rotation mode, the left flap is the prevailing response in this instance. Additionally, the winglets also exhibited the same behavior for these two mode shapes. The asymmetries of the airplane were not unique to one particular setup and were seen throughout all of the test configurations, indicating how the airplane was fabricated and assembled may have played a role in these responses that were seen from the GVT.

Figure 19: Ground vibration test airplane mode shapes for the free-free stab counterweight off setup shown in the order presented from Table 3

4.3 Motor Assembly Results

When gathering the GVT data for the electric motor modes for both the free-free and on-tires setups, all control surfaces were locked in addition to the yoke and pedals in the cockpit. However, the stab counterweight block was installed during the shaker test runs performed on the motors. Post-processing of the test run motor assembly data was a bit tedious as motion from both the wing and the control surfaces in the mode shapes tended to dominate any motion from the motors. Furthermore, smaller frequency range parameter estimations had to be performed as larger frequency ranges did not pick up the motor assembly modes as well.

The motor mode frequencies were much lower than anticipated based on pre-test FEM modal analysis results. For both setups, the lateral and vertical motor assembly modes fell within a frequency range of 29-35 Hz as shown in table 4, and a frequency difference of over 5-percent magnitude are highlighted in red. For the free-free setup, the lateral motor modes appeared more flexible and frequency ranges were lower than the vertical motor modes. On the other hand, for the on-tires setup the anti-symmetric motor lateral mode was the exception as it rather appeared as the last mode of the four motor assembly modes, contributing at a nearly 17-percent difference when compared to the free-free case. The differences between the setups for the other motor assembly modes were fairly small in frequency magnitude. The pre-test FEM did predict higher second-order lateral and vertical motor modes, but because of tight clearance issues and limited real estate around the motors during the GVT setup, additional accelerometers were not installed to capture these higher-order modes. Currently, these lateral and vertical first-order motor assembly modes are the concern for whirl flutter analyses.

Table 4: Frequency comparison table between free-free and on-tires ground vibration test setups for the motor assembly modes

Motor Mode Description	Free-Free Damped Frequency (Hz)	On-Tires Damped Frequency (Hz)	% Difference from Free-Free
Anti-Sym Motor Lateral	29.77	34.85	17.06%
Sym Motor Lateral	30.03	29.70	-1.08%
Anti-Sym Motor Vertical	34.28	33.43	-2.50%
Sym Motor Vertical	34.38	34.43	0.16%

Figure 20 shows the lateral motor mode shapes for the free-free setup, likewise, figure 21 shows the vertical motor mode shapes. Asymmetries were also present between both the left and right motors as one motor assembly tended to dominate over the other -- similar to the airplane mode shapes. The shapes shown in figure 20 evidently show that the left motor assembly is the more dominant one of the two for both the anti-symmetric and symmetric motor assembly vertical modes. The airplane control surfaces, noticeable in figure 21, are dominating the vertical motor mode shapes even though the aileron gust locks were installed to try to help minimize the control surface motion while focusing on the motors.

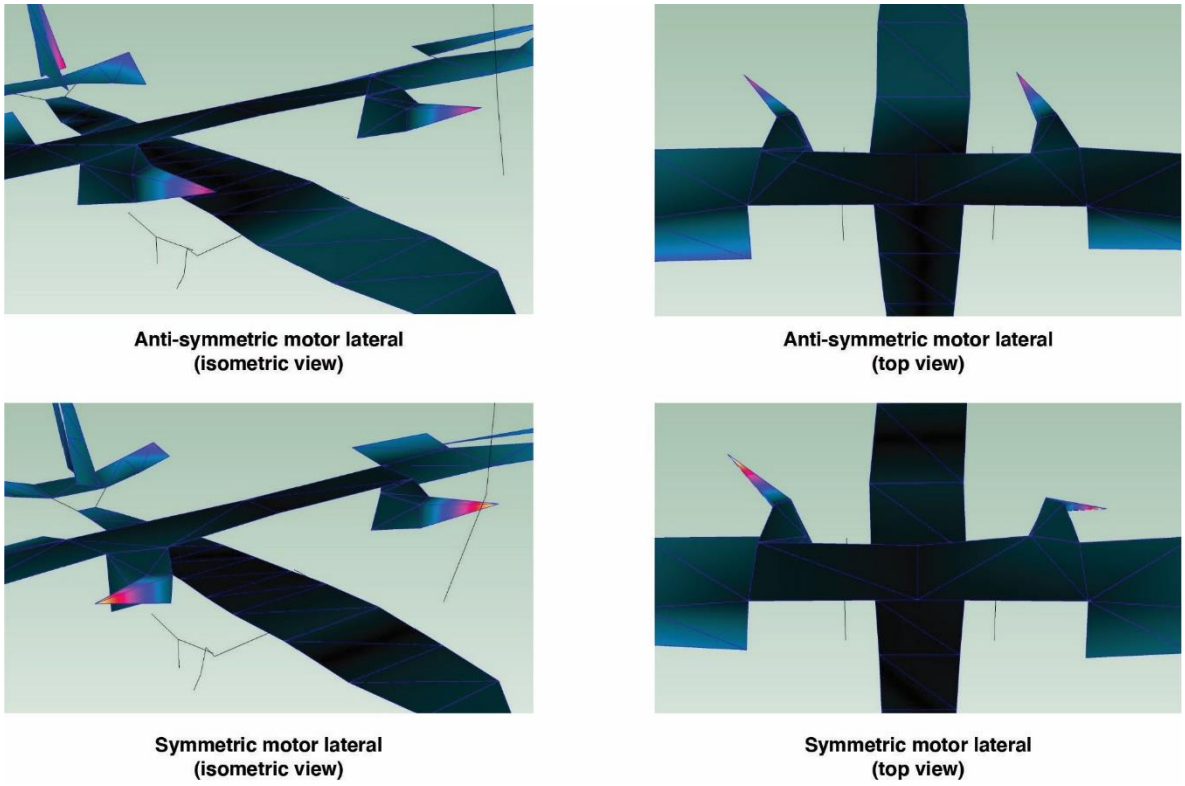

Figure 20: Ground vibration test lateral motor assembly mode shapes for the free-free setup

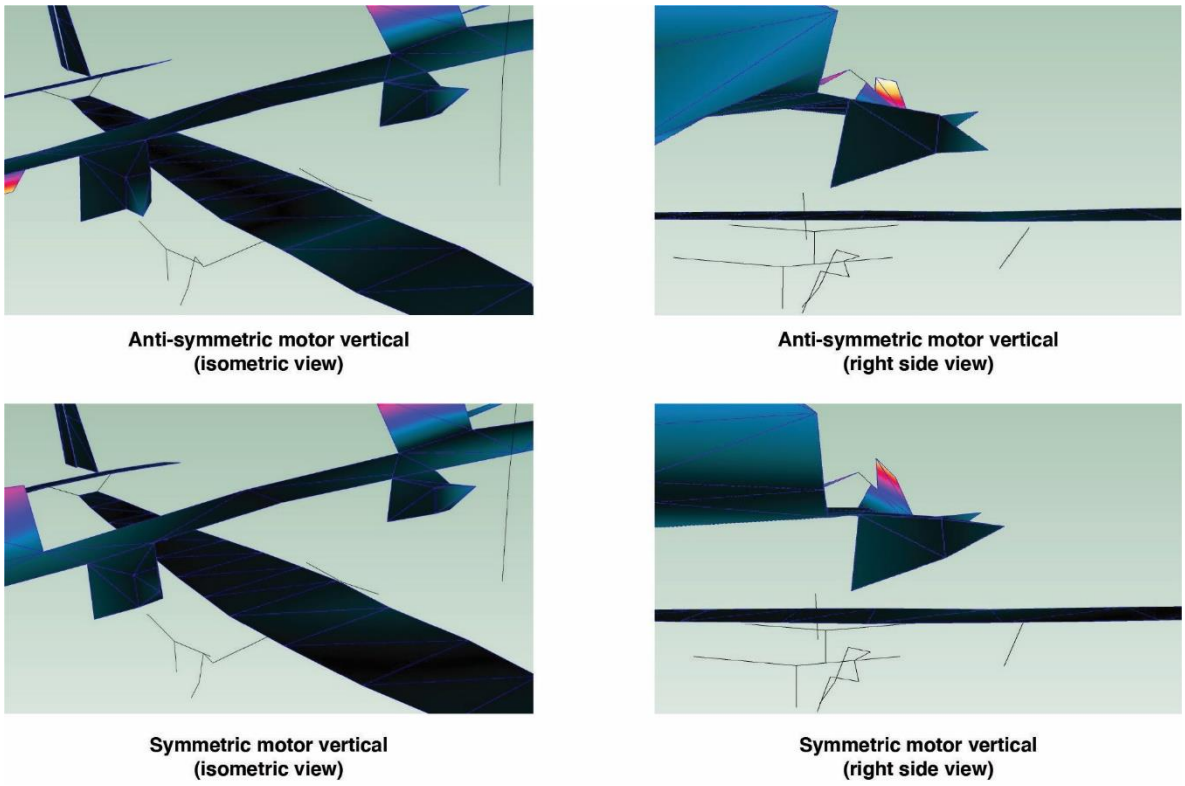

Figure 21: Ground vibration test vertical motor assembly mode shapes for the free-free setup

4.4 Airplane Rigid Body Results

Airplane rigid-body tests were performed while the airplane was installed on soft supports in order to identify the approximate frequencies of the six different rigid-body modes and to evaluate the frequency separation between the highest rigid-body mode (1.06 Hz) and the first airplane elastic mode (7.83 Hz). Manual pushes or excitations were provided from one of the test engineers, and shakers were not used for the rigid-body tests. Figure 22 shows an example of the airplane manual excitation locations used for the rigid-body roll and rigid-body fore/aft modes.

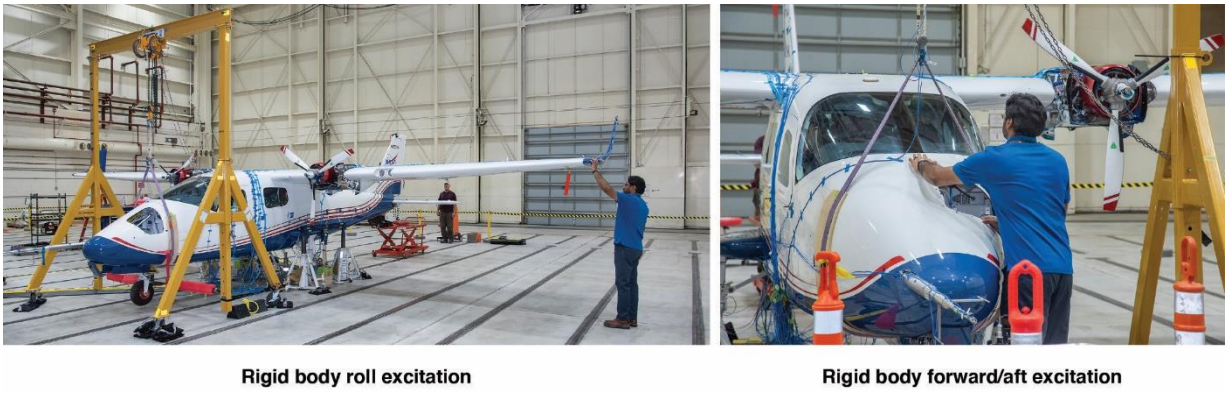

Figure 22: Example of manual excitation locations for some of the rigid-body modes

Airplane rigid-body results are dependent on the design of the soft-support system used. For the newly designed X-57 soft-support system, the rigid-body plunge/bounce mode (1.06 Hz) was of the greatest interest because of the rigid-body mode required to evaluate the frequency separation between the first airplane elastic mode (7.83 Hz). For the X-57 Mod II testing, the 1080HD bungees used in the newly designed soft supports provided a 7x frequency separation (more than adequate for reliable modal data gathered on soft supports). During the manual excitation, there was difficulty getting the airplane to respond to only a single rigid-body mode. Usually the target rigid-body mode would couple with the single rigid-body mode. For example, when trying to excite the fore/aft mode, a gentle push was applied at the fuselage nose, resulting in a coupled fore/aft and pitching motion response from the airplane. Of the six rigid-body modes, the fore/aft, plunge/bounce, and lateral excitations proved a bit difficult. Frequency results for the rigid-body test are shown in table 5.

Table 5: Rigid-body frequency results for the X-57 Mod II airplane suspended on soft supports using bungees

Rigid Body Mode	Average Damped Frequency (Hz)
Rigid Body Yaw	0.47
Rigid Body Lateral	0.53
Rigid Body Fore/Aft	0.68
Rigid Body Pitch	1.00
Rigid Body Roll	1.05
Rigid Body Plunge/Bounce	1.06

SUMMARY

The X-57 Mod II GVT results greatly expanded a better understanding of the modal characteristics of the airplane. The test showed that the pre-test Mod II FEM did not capture all the modes that were observed. In order to capture all the GVT modes in the FEM, the post-test FEM update and model correlation process will be a challenging endeavor for the X-57 project team. In addition, some asymmetries were seen between the left and right sides of the airplane which were noticeable in the control surfaces and the motor assembly. Aside from a few modes being higher than five percent, frequency variations (for the most part) were minimal between the free-free and on-tires setups; however, the on-tires setup did show some coupling in some modes that were not seen in the free-free case. Both the on-tires and free-free GVT set of results will be useful in the control room during taxi testing and envelope-expansion flights of the X-57 Mod II airplane. The follow-on tasks include updating the Mod II airplane FEM to match the GVT results, running both the classical and whirl flutter analyses to verify the flight envelope flutter margins and airworthiness verification of the airplane, and prepping for the Mod II flight-testing.

ACKNOWLEDGEMENTS

The authors thank the X-57 project team and crew as well as the NASA AFRC FLL mechanics and technicians for assisting with the test setup and test conduction. The authors also thank Doug Lovelace from Hottinger Brüel & Kjær for his on-site assistance and support during the test.

REFERENCES

[1] NASA Armstrong Fact Sheet: NASA X-57 Maxwell, https://www.nasa.gov/centers/armstrong/news/FactSheets/FS-109.html, accessed November 9, 2020.

[2] Borer, Nicholas K., Geuther, Steven C., Litherland, Brandon L., and Kohlman, Lee, "Design and Performance of a Hybrid-Electric Fuel Cell Flight Demonstration Concept," AIAA 2018-3357, June 2018, DOI: 10.2514/6.2018-3357

[3] Armstrong Flight Loads Lab, https://www.nasa.gov/centers/armstrong/research/Facilities/FLL/index.html, accessed November 9, 2020.

[4] National Aeronautics and Space Administration, "Flight Demonstrations and Capabilities (FDC) Scalable Convergent Electric Propulsion Technology and Operations Research (SCEPTOR)," Critical Design Review," Edwards, CA, November 2016, https://www.nasa.gov/sites/default/files/atoms/files/sceptor_cdr_day_1_package.pdf, and https://www.nasa.gov/sites/default/files/atoms/files/sceptor_cdr_day_2_package.pdf, accessed November 9, 2020.

[5] Heeg, Jennifer, Stanford, Bret K., Wieseman, Carol D., Massey, Steven J., Moore, James, Truax, Roger, and Miller, Kia, "Status Report on Aeroelasticity in the Vehicle Development for X-57 Maxwell," AIAA 2018-3487, June 2018, DOI: 10.2514/6.2018-3487.

[6] Heeg, Jennifer, Stanford, Bret K, Kreshock, Andrew, Shen, Jiawei, Hoover, Christian, and Truax, Roger, "Whirl Flutter and the Development of the NASA X-57 Maxwell," IFASD-2019-056, June 2019.

[7] Costruzioni Aeronautiche TECNAM srl, Aircraft Maintenance Manual, Doc. No. 2006/045, 2nd Ed – Rev. 2, Italy, September 29, 2012.

[8] "BK Connect® User's Help Guide Version 2019," Brüel & Kjær, Nærum, Denmark, 2019.

[9] Vold, H., J. Kundrat, G.T. Rocklin, and R. Russel, "A Multi-Input Modal Estimation Algorithm for Mini-Computers," SAE International 820194, February 1982, DOI: 10.4271/820194.